

Comparing Group Sparse Reconstruction of 4D EP-COSI data with Compressed Sensing, Total Variation, and Maximum Entropy Reconstruction

Brian L Burns¹, Neil Wilson², and M Albert Thomas^{1,2}

¹Department of Biomedical Engineering, UCLA, Los Angeles, CA, United States, ²Department of Biomedical Physics, UCLA, Los Angeles, CA, United States

Intended Audience: Researchers working in sparse image reconstruction and multidimensional spectroscopic imaging.

Purpose: The Echo-Planar Correlated Spectroscopic Imaging (EP-COSI) sequence allows for the simultaneous acquisition of two spatial (k_y, k_x) and two spectral (t_2, t_1) dimensions in a single scan [1]. The total acquisition time is directly proportional to the number of phase increments in the k_y and t_1 dimensions and can take 20 to 40 minutes depending on the choice of parameters, which is too long to be used clinically. Non-uniform under-sampling (NUS) of the 4D EP-COSI k_y - t_1 plane and reconstructing the missing samples with either Compressed Sensing (CS), Total Variation (TV) denoising, or Maximum Entropy (MaxEnt) has been shown to be a viable way to reduce EP-COSI scan times up to 5X while preserving the spatial-spectral resolution [2,3]. The current work uses the Group Sparse (GS) reconstruction method with overlapping or non-overlapping groups to reconstruct phantom 4D EP-COSI data at different NUS rates using the Split-Bregman (SB) iterative reconstruction algorithm and compares the reconstruction results to CS, TV, and MaxEnt [4,5,6].

Methods: GS reconstruction is a variant of CS that uses a mixed $l_{1,2}$ -regularizer, which reconstructs groups of samples instead of individually [4,7]. The SB algorithm has been modified to solve the GS problem and allows for arbitrary overlapping or non-overlapping groups and can successfully reconstruct NUS 4D EP-COSI data at NUS rates as high as 8X. The k_y - t_1 plane of a phantom 4D EP-COSI scan was retrospectively under-sampled 4X and 8X then reconstructed using either CS, TV, MaxEnt, or GS with 50% overlapping or non-overlapping groups, GS₁ and GS₂, respectively. CS, TV, and GS were reconstructed using a variant of the SB algorithm, and MaxEnt was reconstructed using the Cambridge algorithm [3]. The GS SB algorithm iteratively solves the constrained convex problem:

$$\min_{u,z} \|z\|_{1,2} \text{ s.t. } RF^{-1}u = f \text{ and } z = Gu$$

where u is the reconstructed data, F^{-1} is the 4D Fourier operator, R is the under-sampling mask of the k_y - t_1 plane, f is the sampled data, G is the group matrix of 1s and 0s that determines which coefficients from u belong to each group in z [6], and z contains the reconstruction for every grouping of u .

The group sizes used in GS₁ and GS₂ were $(t_1, t_2) = (4,16)$, which were empirically determined. The CS problem was solved by making the group size one coefficient, $(t_1, t_2) = (1,1)$. The 500ml gray matter brain phantom contained *in vivo* concentrations of NAA, NAAG, GABA, Asp, Cho, Cr, Glc, Glx, Gsh, ml, Lac, and PCh. The 4D EP-COSI scan was acquired on a Siemens 3T Trio scanner: 12 channel head coil, 2x2x2 cm³ voxels, 100 t_1 increments, TR/TE/avg = 1.7s/23ms/1, 32cm x 32cm FOV, and spectral bandwidths of $F_1=1250$ Hz and $F_2=1190$ Hz.

Results: Figure 1 shows a select 2D voxel from the fully sampled 4D EP-COSI phantom scan, the 8X NUS data, and the CS, TV, MaxEnt, GS₁, and GS₂ reconstructions. The 8X NUS spectrum shows significant aliasing along t_1 by the large diagonal peaks, NAA, Cr, Cho, and water, which obscures the low SNR cross peaks of Glx, NAA, ml, and Asp. In each of the reconstructions, the aliasing has been removed and the cross peaks are well resolved. The CS and TV reconstructions have higher noise floors than the other reconstructions as well as residual aliasing from the large water peak. The GS₁, GS₂, and MaxEnt reconstructions all show a reduced noise floor compared to the fully sampled spectrum with distinct cross peaks, however, the GS₁ cross peaks and diagonals are more qualitatively similar to the fully sampled spectrum. Table 1 shows the mean metabolite RMSEs of the reconstructions at 8X and 4X NUS, which were calculated over the metabolite peak locations of the central 3x4 voxels. As shown, GS₁ has the lowest mean RMSE values for almost all of the metabolites for both 4X and 8X NUS with MaxEnt having slightly better values for Lac and Cr.

Discussion: The mean metabolite RMSEs are affected by peak amplitude, line shape, and noise, whereby, lower values correspond to more accurate reconstructions of the fully sampled data. Therefore, GS₁ produced reconstructions that were qualitatively and quantitatively superior to the other methods for large diagonal peaks as well as small cross peaks close to the noise floor.

Conclusion: This pilot study shows that GS reconstruction of NUS 4D EP-COSI data sets is a viable alternative to CS, TV, and MaxEnt reconstructions. The GS SB algorithm was developed and evaluated on phantom data sets at 8X and 4X NUS rates. GS reconstruction results demonstrated better metabolite peak reproduction and lower non-linearity than CS, TV, and MaxEnt with GS₁ providing the best results overall. Further work is required to determine the optimal grouping strategy under *in vivo* experimental conditions.

References – [1] S Lipnick et al, Magn. Reson. Med. 64 (2010):947-956 [2] JK Furuyama, et al, Magn. Reson. Med, 67(2012)1499-1505 [3] BL Burns et al, NMR in Biomed, (2013) in press. [4] M Yuan et al, Statist. Soc. B, 68(2006):49-67 [5] T Goldstein et al, SIAM J. Imaging Sci.,(2009):323-343 [6] D Wei et al, TR11-06, Tech. Rep., Rice U., 2011. [7] M Lustig et al, Magn. Reson. Med. 58.6(2007):1182-1195

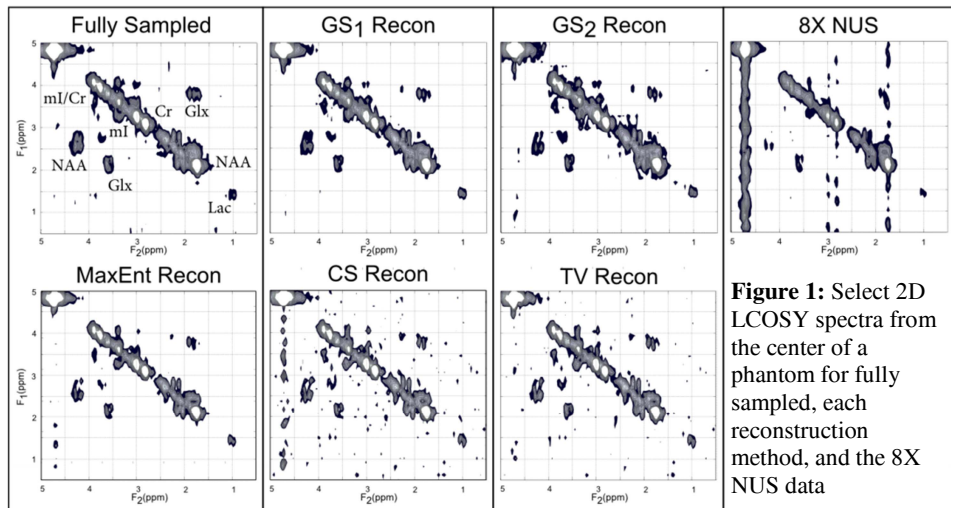


Figure 1: Select 2D LCOSY spectra from the center of a phantom for fully sampled, each reconstruction method, and the 8X NUS data

$\times 10^{-6}$	NUS		CS		GS2		GS1		MaxEnt		TV	
	4X	8X	4X	8X	4X	8X	4X	8X	4X	8X	4X	8X
Asp	8.67	11.1	2.61	4.60	2.43	4.39	2.16	4.18	2.26	4.55	2.38	4.42
Cho	6.57	8.62	2.79	3.74	2.62	3.66	2.10	3.17	2.21	3.30	2.51	3.58
Cr	22.3	29.2	4.11	8.48	5.03	8.66	3.75	7.87	3.50	8.04	4.11	8.21
Glx	8.13	8.83	3.06	4.07	2.79	3.76	2.05	3.13	2.37	3.50	2.70	3.96
Lac	3.48	4.37	1.88	2.22	2.11	2.41	1.52	1.87	1.44	1.81	1.73	2.12
Mi	6.72	9.01	3.14	3.80	3.86	4.72	2.32	3.39	2.41	3.42	2.79	4.01
NAA	12.1	15.8	3.49	5.63	3.02	4.99	2.42	4.55	3.04	5.07	3.15	4.94

Table 1: Mean metabolite RMSEs over 3x4 voxels for the NUS and reconstructed data